

Unimolecular Decomposition of Pyruvic Acid: An Experimental and Theoretical Study

Ko Saito,* Goki Sasaki, Kazumasa Okada, and Seiji Tanaka

Department of Chemistry, Faculty of Science, Hiroshima University, Higashi-Hiroshima 724, Japan

Received: October 22, 1993; In Final Form: January 24, 1994*

The thermal decomposition of pyruvic acid diluted in Ar has been studied behind reflected shock waves over the temperature range 850–1000 K, with a total density range of $(0.3\text{--}1.3) \times 10^{-5}$ mol/cm³. The decomposition process was monitored by time-resolved IR emission from carbon dioxide product. The vacuum-UV absorption at 193 nm suggested the production of hydroxyethylidene from the initial decomposition. This carbene isomerizes to acetaldehyde at temperatures higher than those used under the present conditions. From the experimental results, we propose that the initial reaction occurs through a five-center transition state (TS) as $\text{CH}_3\text{COCOOH} \rightarrow \text{CH}_3\text{COH} + \text{CO}_2$ with a rate constant $k = 10^{12.46} \exp(-40.0 \text{ kcal mol}^{-1}/RT) \text{ s}^{-1}$. An ab initio molecular orbital calculation at the HF/6-31G**//HF/3-21G level shows that the energy of the five-center TS producing hydroxyethylidene is lower by 60 kcal/mol than that of the four-center TS leading directly to acetaldehyde. A theoretically evaluated rate constant agrees with the experimental value, in support of the proposition that the reaction path occurs through the five-center TS to produce the carbene radical. Also, it appears that the carbene subsequently isomerizes through two routes leading to acetaldehyde and/or vinyl alcohol.

1. Introduction

Kinetic investigations of pyruvic acid decomposition in the gas phase have been reported by Yamamoto and Back¹ and by Taylor.² According to Yamamoto and Back, the UV photolysis of pyruvic acid produced CO₂ and hydroxyethylidene (hydroxymethylcarbene) through a five-center transition state (TS). On the other hand, in the thermal decomposition using a static system, they proposed that the reaction proceeds through a four-center TS which directly gives CO₂ and acetaldehyde. They evaluated Arrhenius parameters as $\log(A/\text{s}^{-1}) = 7.19$ and $E_a = 27.7$ kcal/mol in the temperature range 455–584 K. Taylor measured the decomposition rate by observing the total pressure change during the course of the reaction and obtained $\log(A/\text{s}^{-1}) = 13.53$ and $E_a = 41.25$ kcal/mol for 556.8–607.4 K. He assumed the molecular decomposition process to give only CO₂ and acetaldehyde. The Arrhenius parameters of these previous studies differ from each other even though the rate constants are equal at around 500 K. Just as in the photolysis, Yamamoto and Back reported that, in the thermal reaction, the ratio of the products, [acetaldehyde]/[CO₂], was less than unity at pressures higher than 1 Torr. However, they did not explain this experimental result and the unusually low frequency factor in their Arrhenius expression.

Because of the above disagreements, we have attempted in the present work to measure the initial decomposition rate using the shock tube method. With this technique, complications due to heterogeneous reactions can be avoided to a considerable extent. Also, in order to corroborate the decomposition mechanism, we have calculated possible transition-state structures by an ab initio MO method.

2. Experimental Section

A time-resolved spectroscopic study was performed in a 9.4-cm-i.d. pressurized driver shock tube. Detailed descriptions of the shock tube equipment and the optical system are given in previous papers.³ The tube, with a 3.8-m-long drive section, was made of stainless steel. It was routinely pumped down by a liquid nitrogen trapped 6-in. diffusion pump to less than 2×10^{-6} Torr. Three pressure transducers were mounted on the shock tube walls 160 mm apart from one another near the end of the drive section.

The signals from these transducers were used to trigger a transient digital recorder and a universal counter. The shock conditions for each run were calculated from the measured shock speed on the basis of the shock relations for the ideal gas. The error of the shock speed measurement was less than 1% which induced maximum errors of ca. 2% in the temperature and 1.3% in the density behind the reflected shocks. The experimental conditions for the present kinetic analysis were as follows: temperature = 850–1000 K, total density = $(0.3\text{--}1.3) \times 10^{-5}$ mol/cm³, reactant concentrations = 0.07–0.24 mol % in Ar. The boundary layer effects were considered under the present conditions, and the experimental Arrhenius parameters were corrected as described later.

The optical system used for the vacuum-UV absorption was constructed as follows. The resonance radiation of carbon atoms (180 and 193 nm) was produced by microwave excitation of He containing a few percent methane flowing in a quartz tube at about 10 Torr. The radiation from the lamp passed through two MgF₂ windows (1.0-mm thickness) mounted on the shock tube walls at a position 2 cm from the end plate, and the light through the windows was focused into a vacuum-UV monochromator. A photomultiplier (HTV-R431s) operating at 1 kV was used to detect the light intensity. The time constant of the optical-electrical system was about 10 μs with an S/N ratio of about 10.

Carbon dioxide which is produced from the initial reaction was monitored by IR emission from the ν_3 band of CO₂. The radiation from the shock-heated gas was passed through a 4.23-μm interference filter with 0.18-μm FWHM and was detected by a HgCdTe element cooled at 77 K. All of the output signals were recorded on a digital storage oscilloscope.

For qualitative identification of the products, the shock-heated gas was expanded into a glass cylinder and injected into a gas sampling cell for GC analysis with a 2-m Porapak-Q column.

3. Computational Methods

Ab initio MO calculations were carried out with GAUSSIAN-82 and -90 program packages.⁴ The geometries of the reactants, products, and transition states were fully optimized by the energy gradient method. All optimized geometries were determined with the HF/3-21G basis set. Vibration frequencies were calculated by using analytical second derivatives, at the HF/3-21G level, to confirm all stationary point structures and to correct for zero-

* Abstract published in *Advance ACS Abstracts*, March 1, 1994.

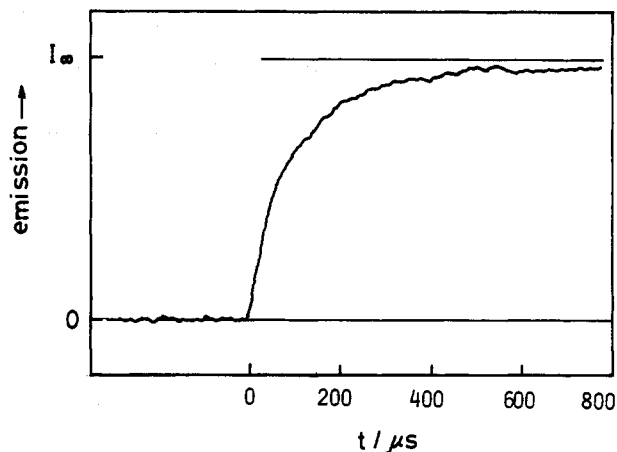


Figure 1. Typical emission profile at 4.23 μm . Conditions: $T = 950 \text{ K}$, total density = $0.9 \times 10^{-5} \text{ mol/cm}^3$, 0.14 mol % reactant in Ar.

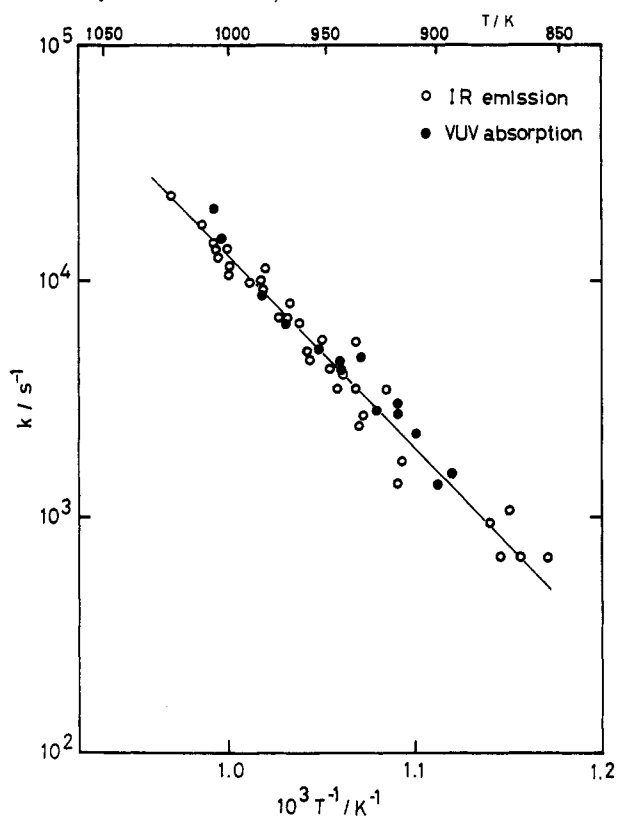


Figure 2. Arrhenius plot of the rate constant for the CO_2 production (open circles) and for the VUV absorption (closed circles).

point vibrational energy levels. For the evaluation of the total energies, Møller–Plesset perturbation calculations (MP2)⁵ were executed in the 6-31G** basis set in order to account for the effects of electron correlation. Theoretical rate constants were evaluated for the possible reaction channels with conventional transition-state theory (TST).⁶

4. Results and Discussion

A. Experimental Results. Figure 1 shows a typical emission profile at 4.2 μm . Preliminary experiments revealed that the emission intensity was proportional to the concentration of carbon dioxide. The time history of the intensity was expressed as $I = I_\infty [1 - \exp(-kt)]$, where k is the first-order rate constant of the CO_2 production. Figure 2 shows an Arrhenius plot of k values for typical initial conditions. It was found that the first-order rate constants thus obtained are essentially independent of the reactant concentration and the total density, suggesting that the decomposition is in the high-pressure limit.

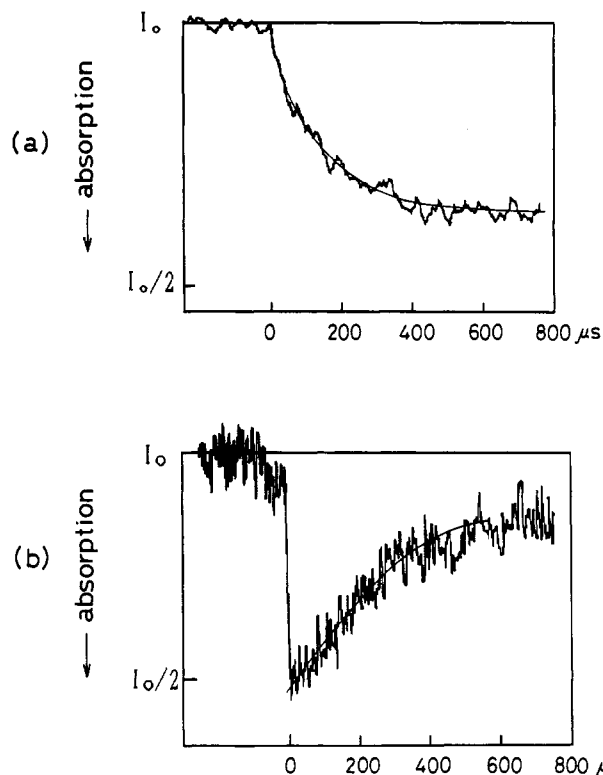


Figure 3. Typical absorption traces at 193 nm. (a) Conditions: $T = 940 \text{ K}$, total density = $0.9 \times 10^{-5} \text{ mol/cm}^3$, 0.13 mol % reactant in Ar. (b) Conditions: $T = 1310 \text{ K}$, total density = $1.1 \times 10^{-5} \text{ mol/cm}^3$, 0.16 mol % reactant in Ar.

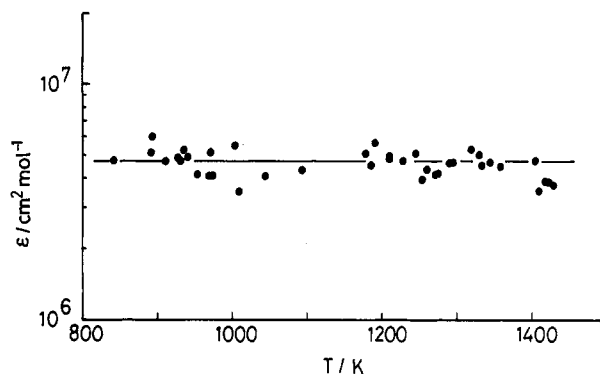


Figure 4. Plot of absorption coefficients for a product at 193 nm which was produced from the decomposition of pyruvic acid. Average value is $(4.7 \pm 0.5) \times 10^6 \text{ cm}^2/\text{mol}$.

There was no apparent absorption by the reactant in the VUV region (180 and 193 nm) under the present conditions. At room temperature the absorption coefficient of pyruvic acid is too small to be measured at 1 Torr with an optical path length of 10 cm.⁷ This fact was confirmed in the present study. At high temperatures around 1000 K, the absorption coefficient was estimated to be less than $6 \times 10^5 \text{ cm}^2 \text{ mol}^{-1}$, and this gave negligibly small absorbance under the present conditions. On the other hand, a large absorption due to some product was observed. Figure 3a shows a typical absorption trace at 193 nm and 940 K. The trace shows a slow increase of absorption beginning at the reflected shock front. With increasing temperature the initial rise became faster, and after it reached a maximum the absorption gradually decreased. At temperatures higher than the present work the absorption trace rose abruptly and then decreased rapidly as shown in Figure 3b at 1310 K. This absorption behavior suggests that the absorbing species is an intermediate which disappears after most of the reactant has been consumed. The same behavior was observed at 180 nm as well.

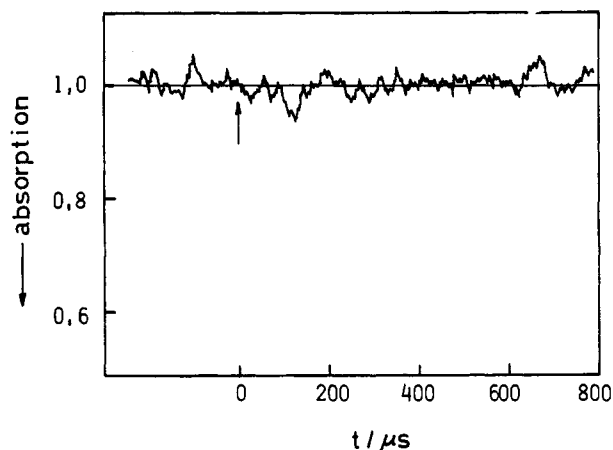


Figure 5. Absorption trace at 193 nm for acetaldehyde. Conditions: $T = 935$ K, total density = 0.9×10^{-5} mol/cm³, 0.50 mol % acetaldehyde in Ar. Arrow indicates the reflected shock front.

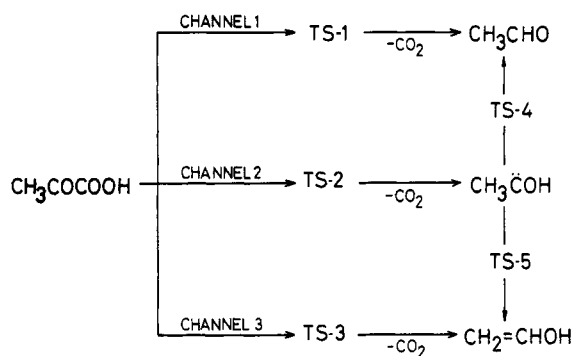


Figure 6. Reaction scheme of the unimolecular decomposition of pyruvic acid.

On the assumption that one molecule of intermediate is formed for every molecule of pyruvic acid decomposed, the absorption coefficient (base e) of the intermediate was $(4.70 \pm 0.5) \times 10^6$ cm²/mol at 193 nm. Temperature dependence over the range

840–1430 K was not observed as shown in Figure 4. Rate constants for the increase of the product were evaluated from absorption traces and are plotted in Figure 2 together with those obtained from the IR emission profile. It appears that there is no systematic difference between the rate constants obtained from the two methods. The scatter of the data at a given temperature is within a factor of 2. A least-squares treatment of these data gives Arrhenius parameters as $\log(A/s^{-1}) = 12.44$ and $E_a = 38.1$ kcal/mol. If we take into account the boundary effects on the thermodynamic conditions in the reflected region, the effects cause a $\sim 5\%$ underestimation in the A -factor and E_a under the present experimental conditions. Thus, we evaluate the Arrhenius expression after the correction as

$$k = 10^{12.46} \exp(-40.0 \text{ kcal mol}^{-1}/RT) \text{ s}^{-1}$$

The probable initial products are carbon dioxide, acetaldehyde, and its isomers such as oxylene, vinyl alcohol, and hydroxyethylidene.^{1,2} At temperatures higher than 1500 K the absorption from the $v = 1$ level of CO₂ was observed at 193 nm.⁸ However, since the absorption coefficient is low, 6×10^5 cm²/mol at 1500 K, the contribution of CO₂ is negligible in the present study. According to a recent work, it was shown that there are absorption bands of acetaldehyde in the vacuum-UV region.⁹ To examine the absorption by acetaldehyde, an additional absorption experiment was performed with acetaldehyde at 180 and 193 nm. Mixtures of acetaldehyde (0.5 mol %) and paraldehyde (0.13 mol %), diluted in Ar, were shock heated to about 1000 K, but absorption was not observed behind the reflected shock waves at these wavelengths, as shown in Figure 5. That is, the absorption coefficient of acetaldehyde is estimated to be less than 5×10^5 at these wavelengths. In a previous study, we confirmed that acetaldehyde and also the acetaldehyde produced from paraldehyde are stable such that the half-life of acetaldehyde is greater than 1 s at 1400 K.¹⁰ Therefore, if the observed absorption in the decomposition of pyruvic acid were due to acetaldehyde, the absorption should not decrease in the observation time, as shown in Figure 3b. Moreover, as described later, it is impossible to energetically form vinyl alcohol and oxylene directly in the first

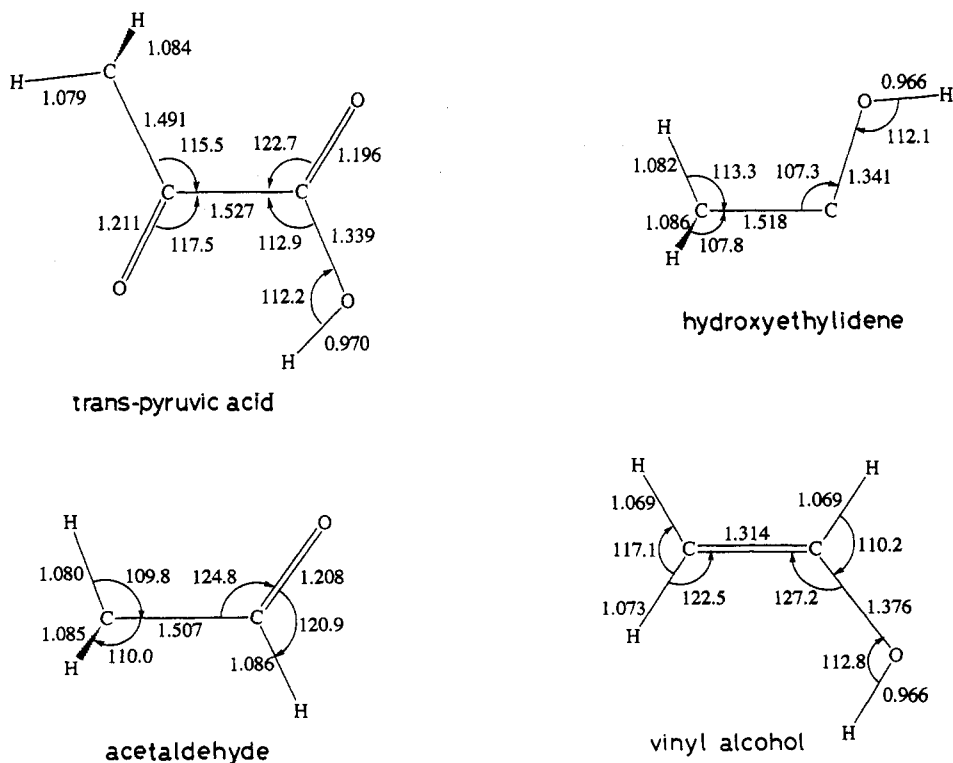


Figure 7. HF/3-21G optimized geometries for the reactant and the products.

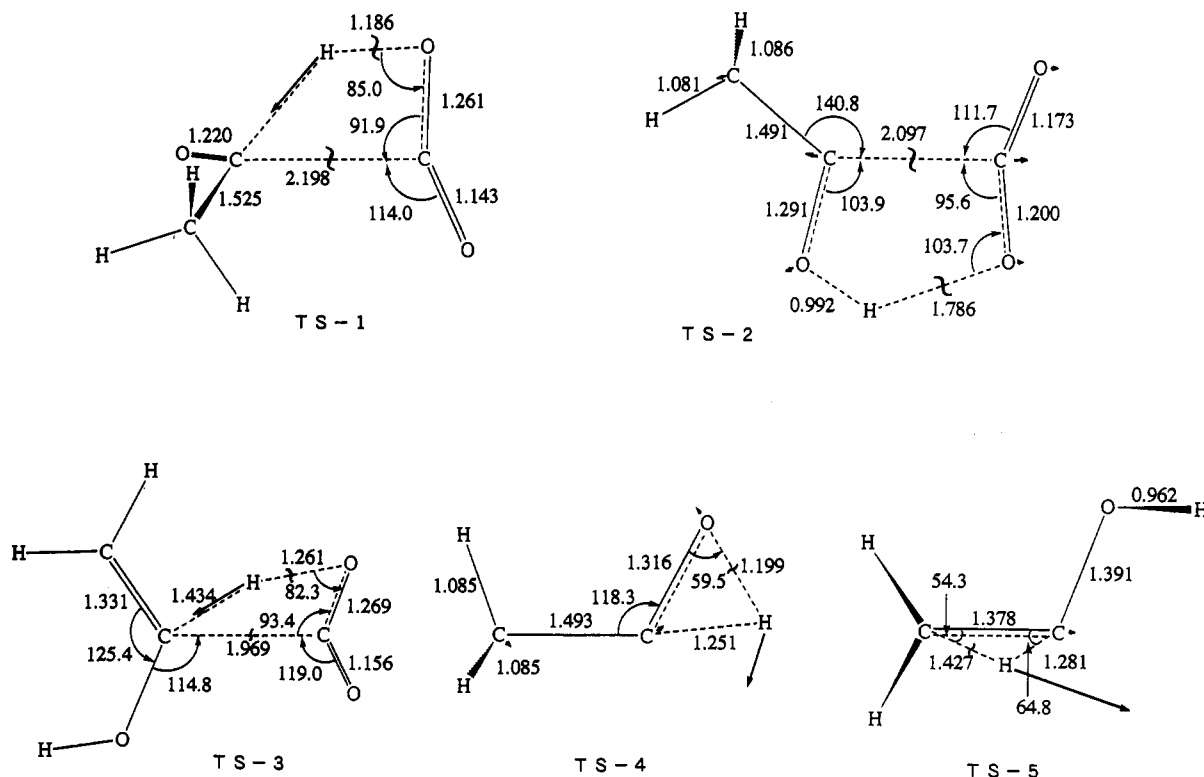


Figure 8. Optimized geometries for transition states of each reaction path.

TABLE 1: Total Energies (hartrees) and Relative Energies (in Parentheses, kcal/mol) Relative to *trans*-Pyruvic Acid with Zero-Point-Energy Correction^a

<i>trans</i> -pyruvic acid -341.53931 (0.0)	acetaldehyde -340.55506 ^b (-13.0)	hydroxyethylidene -340.47534 ^b (36.2)	vinyl alcohol -340.53287 ^b (1.5)	carbon dioxide -187.63342
TS-1 -340.36851 (100.9)	TS-2 -340.47091 (40.8)	TS-3 -340.36204 (105.9)	TS-4 -340.39729 ^b (81.4)	TS-5 -340.41690 ^b (70.4)

^a HF/6-31G** at HF/3-21G-optimized geometries. ^b Energies include that of carbon dioxide.

step. From these facts, the vacuum-UV absorption observed in the pyruvic acid decomposition cannot be attributed to these stable products. Theoretical calculations described later show that hydroxyethylidene is the most probable product in the first step of the decomposition. However, in the GC analysis of the shock-heated gas, acetaldehyde was detected as one of the main products. It is likely that the carbene produced in the first step isomerizes either in a consecutive gas-phase reaction or heterogeneously on the shock tube walls long after the experiment is completed.

B. Calculated Results. There have never been any reported theoretical studies on the thermal decomposition of pyruvic acid. Figure 6 shows an assumed reaction scheme including intermediates and sequences of possible elementary conversions. Three channels are considered: channel 1 leads directly to acetaldehyde through a four-center transition state (TS-1), channel 2 leads to hydroxyethylidene through a five-center transition state (TS-2), and channel 3 leads to vinyl alcohol through a four-center transition state (TS-3). In the channel 3 case, TS-3 is formed from the enol form ($\text{CH}_2=\text{COHCOOH}$) and is higher lying than the keto acid by 12 kcal/mol (HF/6-31G**). There are two conformations for TS-1 corresponding to different symmetries, C_s and C_1 , with nearly the same energy. The carbene produced from channel 2 isomerizes to acetaldehyde through TS-4 or to vinyl alcohol through TS-5.

Figure 7 shows geometries of the reactant and products (acetaldehyde, vinyl alcohol, hydroxyethylidene) optimized at the HF/3-21G level. The *trans* form of pyruvic acid is more stable than the *cis* form by 11.7 kcal/mol at the MP2/3-21G level. Figure 8 shows the fully optimized HF/3-21G geometries

of the transition states and the displacement vectors of the normal modes with imaginary vibrational frequencies. Table 1 is a summary of total and relative energies with respect to *trans*-pyruvic acid for these species. All of the fully optimized geometries were confirmed to have only one imaginary vibration corresponding to the reaction path.

A schematic potential diagram for the decomposition of pyruvic acid is shown in Figure 9 for channels 1 and 2 and in Figure 10 for channel 3, respectively. The relative energies indicated are the results of the HF/6-31G**//HF/3-21G calculations with the zero-point-energy (ZPE) corrections. It appears that the lowest potential barrier among the possible initial reactions is the path to give hydroxyethylidene and CO_2 through a five-center transition state (TS-2). The remaining channels, which directly produce acetaldehyde and vinyl alcohol, have higher potential energy barriers. With the present calculational level, these transition states are higher than TS-2 by about 60 and 65 kcal/mol, respectively. Although these energy differences depend on the calculational method, a large decrease of these potential barriers using more sophisticated methods is not to be expected. With transition-state theory, Arrhenius parameters for channel 2 were evaluated for comparison with the experimental values. This calculation of course assumes that the reaction is in the high-pressure limit.

C. Initiation Process. Figure 11 shows a comparison of the rate constants obtained in the present work with those measured at low temperatures and also with the above-mentioned theoretical values. Previous investigations for the decomposition have been carried out using static systems. Yamamoto and Back proposed

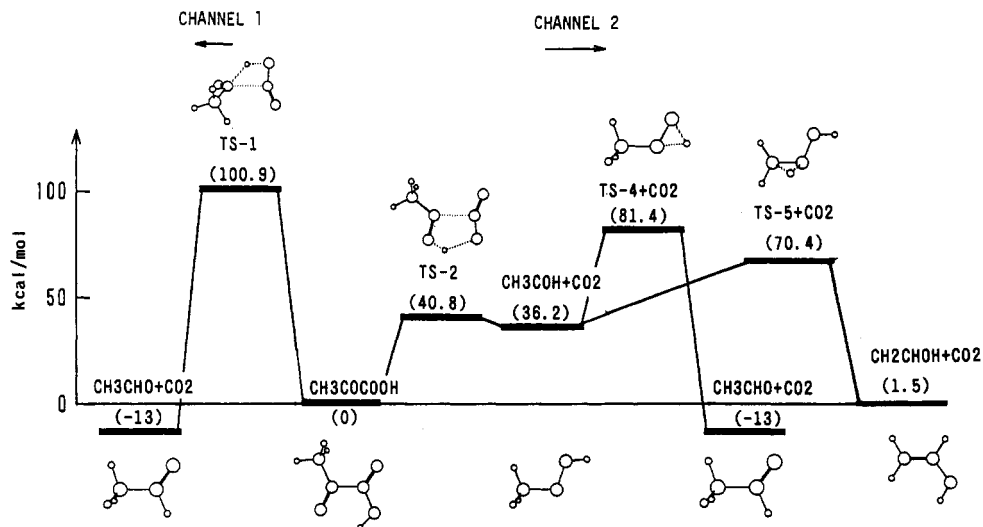


Figure 9. Relative potential energies for channels 1 and 2. Energies are evaluated at the HF/6-31G**//HF3-21G level. Relative values are corrected by ZPE (zero point energy).

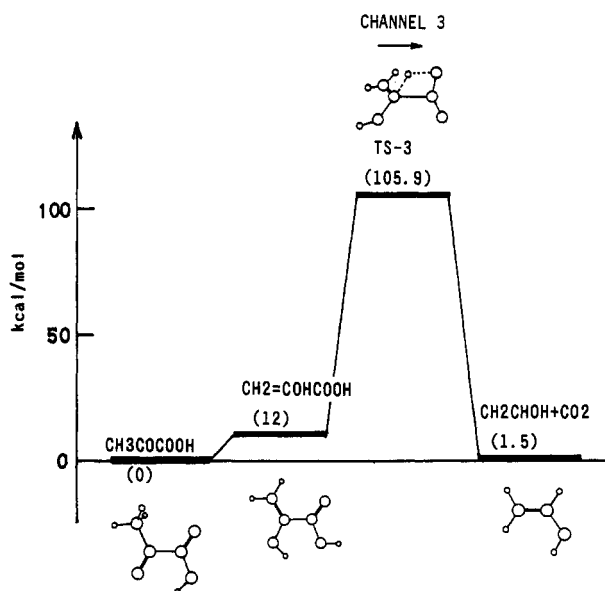


Figure 10. Relative potential energies for channel 3. Indicated values are the same as in Figure 9.

that initiation in the UV photolysis involved fragmentation into carbon dioxide and hydroxyethylidene.¹ On the other hand, they assumed that the thermal decomposition gave acetaldehyde through a four-center TS directly instead of the carbene. However, their yield of acetaldehyde was always lower than that of carbon dioxide. Taylor proposed, for the thermal reactions of a series of substituted compounds of pyruvic acid, that the decomposition also proceeds through a four-center TS to give CO₂ and aldehydes.¹¹ He also explained the relative decomposition rates of these compounds as being due to charge-induced effects. His proposal was reasonable since the relative reactivity showed a linear correlation using the Hammett rule. Therefore, the previous two research groups concluded that the initial process in the thermal decomposition produced aldehyde directly.

In the present study, an MO calculation gave a potential barrier of ~40 kcal/mol for the decomposition into CO₂ and hydroxyethylidene. This should be compared to 100 kcal/mol for the direct production to give acetaldehyde. The low potential energy for the five-center transition state (TS-2) is not surprising if the structure of the intramolecular hydrogen bonding is considered just as in the condensed phase.¹² Thus, the present calculation suggests that the path to give acetaldehyde directly simply cannot occur. Also, channel 3 is likewise negligible due to the high

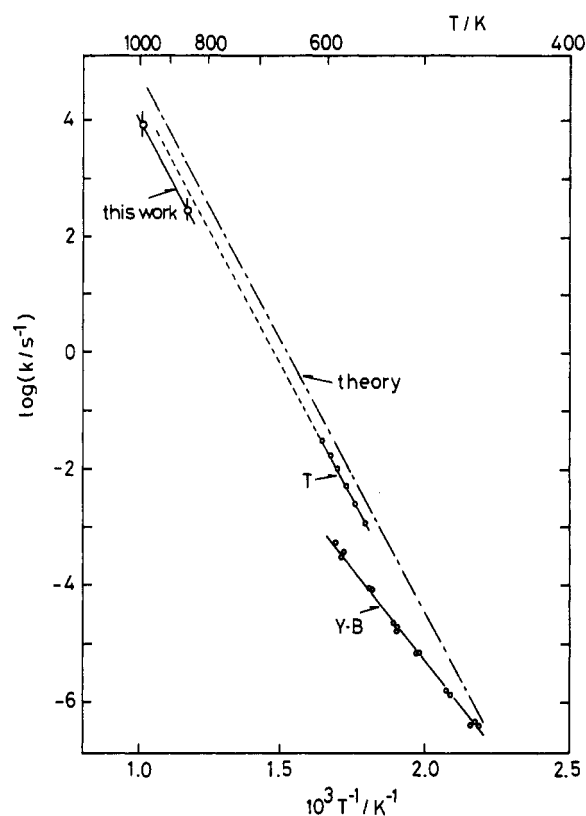


Figure 11. Comparison of the rate constants obtained for the decomposition of pyruvic acid: Y-B, ref 1; T, ref 2.

potential barrier of TS-3. We experimentally detected a product which had strong absorption bands in the vacuum-UV region. However, the absorption of acetaldehyde was ascertained to be negligible under the experimental conditions. The activation energy for the decomposition was 40 kcal/mol, in good agreement with the calculated estimate. Hence, the unknown species produced in the decomposition is almost certainly hydroxyethylidene.

Absorption bands in the vacuum-UV region have been reported for the CH₂ radical.¹³ It is therefore not unreasonable to expect absorption bands for hydroxyethylidene. McLafferty and co-workers reported on the stability of hydroxyethylidene.¹⁴ Their opinion is basically in agreement with the present results. Also, a similar reaction path has been found in the decomposition of

glyoxylic acid.¹⁵ In this case, decomposition produced carbon dioxide and hydroxycarbene through a five-center transition state.

As stated in the Introduction, Yamamoto and Back found that the ratio of the products, [acetaldehyde]/[CO₂], was less than unity at pressures higher than 1 Torr. This can be explained by the fact that some of the carbene initially produced isomerizes to vinyl alcohol, which then polymerizes on the tube walls before the product is analyzed.

5. Conclusion

The thermal decomposition of pyruvic acid diluted in Ar has been studied behind reflected shock waves. The decomposition rate constants were evaluated to be $k = 10^{12.46} \exp(-40.0 \text{ kcal mol}^{-1}/RT) \text{ s}^{-1}$. This is in good agreement with previous results obtained by Taylor, who measured the time dependence of the pressure change in a static system.² The initial decomposition mechanism produces carbon dioxide and hydroxyethylidene which isomerizes to acetaldehyde and/or vinyl alcohol eventually.

Acknowledgment. We thank Professor A. Imamura for his advice on this research. The numerical calculations were carried out at the Information Processing Center of Hiroshima University and the Computer Center of the Institute for Molecular Science. This work is supported, in part, by a Grant-in-Aid for Scientific Research from the Ministry of Education.

References and Notes

- (1) Yamamoto, S.; Back, R. A. *Can. J. Chem.* **1985**, *63*, 549.
- (2) Taylor, R. *Int. J. Chem. Kinet.* **1987**, *19*, 709.
- (3) (a) Saito, K.; Kakumoto, T.; Murakami, I. *J. Phys. Chem.* **1984**, *88*, 1182. (b) Saito, K.; Ito, R.; Kakumoto, T.; Imamura, A. *J. Phys. Chem.* **1986**, *90*, 1422.
- (4) (a) Binkley, J. S.; Frisch, M. J.; Raghavachari, K.; Defrees, D. J.; Schlegel, H. B.; Whiteside, R. A.; Fluder, E. M.; Seeger, R.; Pople, J. A. *GAUSSIAN 82*; Carnegie-Mellon University: Pittsburgh, PA, 1983. (b) Frisch, M. J.; Head-Gordon, M.; Trucks, G. W.; Foresman, J. B.; Schlegel, H. B.; Raghavachari, K.; Robb, M.; Binkley, J. S.; Gonzalez, C.; Defrees, D. J.; Fox, D. J.; Whiteside, R. A.; Seeger, R.; Melius, C. F.; Baker, J.; Martin, R. L.; Kahn, L. R.; Stewart, J. J. P.; Topiol, S.; Pople, J. A. *GAUSSIAN 90*; Gaussian, Inc.: Pittsburgh, PA, 1990.
- (5) (a) Binkley, J. B.; Popole, J. A.; Hehre, W. J. *J. Am. Chem. Soc.* **1975**, *97*, 229. (b) Pople, J. A.; Hehre, W. J. *Int. J. Quantum Chem. Symp.* **1976**, *10*, 1.
- (6) Glasstone, S.; Laidler, J. K.; Eyring, H. *The Theory of Rate Processes*; McGraw-Hill: New York, 1941.
- (7) Hall, G. E.; Muckerman, J. T.; Preses, J. N.; Westone R. E., Jr.; Flynn, G. W. *Chem. Phys. Lett.* **1992**, *1193*, 77.
- (8) Koshi, M.; Yoshimura, M.; Matsui, H. *Chem. Phys. Lett.* **1991**, *176*, 519.
- (9) Bring, P.; O'Toole, L. *J. Chem. Soc., Faraday Trans.* **1990**, *86*, 3349.
- (10) Shimofuji, K.; Saito, K.; Imamura, A. *J. Phys. Chem.* **1991**, *95*, 155.
- (11) Taylor, R. *Int. J. Chem. Kinet.* **1991**, *23*, 247.
- (12) Ray, W. J.; Katon, J. E.; Phillips, D. B. *J. Mol. Struct.* **1981**, *74*, 75.
- (13) Herzberg, G. *Proc. Roy. Soc. A* **1961**, *262*, 291.
- (14) Wesdemiotis, C.; McLafferty, F. W. *J. Am. Chem. Soc.* **1987**, *109*, 4760.
- (15) Kakumoto, T. *J. Sci. Hiroshima Univ., Ser. A* **1987**, *51*, 69.